Articles

Assembly of Colloidal Crystals at Electrode Interfaces

M. Trau,*,† D. A. Saville, and I. A. Aksay

Department of Chemical Engineering and Princeton Materials Institute, Princeton University, Princeton, New Jersey 08544-5263

Received May 30, 1997. In Final Form: July 18, 1997[⊗]

We describe a theory for a new type of colloid behavior whereby particles deposited on a surface by electrophoresis are manipulated to form two-dimensional crystals. Since the particles are equally charged, the clustering is opposite that expected from electrostatic considerations. Such behavior is consistent with migration due to electrohydrodynamic flows associated with polarization layers and ion currents. Provided colloid stability is maintained, the assembly processes take place with both dc and ac fields and may be modulated by adjusting the field strength or frequency. No migration is present at frequencies above 1 MHz. Two-dimensional fluid and crystalline states can be formed on the electrode surface. Experiments with patterned electrodes demonstrate the presence of the electrohydrodynamic flow. A mathematical model of the electrohydrodynamics provides insight into the assembly process.

Introduction

The fabrication of materials with structural features on the 1−1000 nm size scale is a rapidly emerging area in materials science[1,2] because nanostructured, multilayered thin film composites (nanolaminates) exhibit properties remarkably different from conventional engineering materials. Examples include metal−metal and ceramic−metal compositionally modulated nanolaminates for applications as diverse as high-temperature gas turbines,[3] soft X-ray and extreme ultraviolet mirrors,[4] and magnetic materials for high-density magnetic recording and magneto-optical data storage and retrieval.[5] Moreover, it is known that nested levels of structural hierarchy impart superior properties compared to homogeneous materials.[6−9] This design feature is exploited in biological materials (e.g., bone, abalone shell, deer antler, and muscle tissue) where subtle differences on various length scales improve performance. Although nanostructured materials display considerable potential, they are difficult to assemble under ambient conditions. Due to the intrinsic dimensional limitations of mechanical techniques, pattern formation in man-made materials has been restricted to length scales larger than a few tens of micrometers. Although nanolaminates are produced by molecular deposition techniques utilizing individual molecules as building blocks,[3,10] the methods can be cumbersome and costly and usually produce small quantities of material. Alternatively, larger structures could be assembled from macromolecular building blocks (e.g., colloids and proteins) via electrophoretic deposition.

In an earlier paper,[11] we described the assembly of colloidal particles on the surface of an electrode using electrical forces. Electrical manipulation of the assembly allows construction of colloidal films with "designed" microscopic architecture. In our report we advanced the hypothesis that the underlying mechanism was of an electrohydrodynamic nature. The theory is described here, along with additional experiments on the mechanism.

Electrophoresis was discovered in 1807 by Ruess,[12] who noticed particle migration toward the anode upon passing an electric current through a suspension of clay in water. Electrophoretic deposition has long been used in a variety of systems. Metals, oxides, phosphors, inorganic and organic paints, rubbers, dielectrics, superconductors, and glasses have all been deposited electrophoretically from aqueous and nonaqueous media.[13] On the other hand, the assembly of colloids into crystalline structures is usually done by dispersing monosized colloidal particles into a solvent and manipulating particle−particle interaction forces or entropic effects.[14] These are difficult to regulate externally and cumbersome to confine to two dimensions.[15]

Much work to date concerns deposition rates, maximum achievable thickness, and film porosity; less attention is paid to processes influencing the morphology of the

* To whom correspondence should be addressed. E-mail: trau@chemistry.uq.edu.au.

† Now at Department of Chemistry, University of Queensland, Brisbane, Queensland 4072, Australia.

⊗ Abstract published in *Advance ACS Abstracts,* November 1, 1997.

(1) General reviews: (a) Siegel, R. W. *Phys. Today* **1993**, October, 64 and *Nanostruct. Mater.* **1993**, *3*, 1. (b) Whitesides, G. W.; Mathias, J. P.; Seto, C. T. *Science* **1991**, *254*, 1312. (c) Schnur, J. M. *Science* **1993**, *262*, 1669. (d) Andres, R. P.; *et al. J. Mater. Res.* **1989,** *4*, 705.

(2) Specific examples: (a) Masuda, H.; Fukuda, K. *Science* **1995,** *268*, 1466. (b) Wu, C. G.; Bein, T. *Science* **1994,** *266*, 1013. (c) Niihara, K. *J. Ceram. Soc. Jpn.* **1991,** *99*, 974. (d) Siegel, R. W.; Ramasamy, R.; Hahn, H.; Tiang, L.; Gronsky, R *J. Mater. Res.* **1988,** *3*, 1367. (e) Tsakalakos, T.; Hilliard, J. E. *J. Appl. Phys.* **1983,** *54*, 734. (f) Jankowski, A. F. *Nanostruct. Mater.* **1995**, *6*, 179.

(3) Gell, M. *J. Min Met. Mater. Soc. (JOM)* **1994**, *46*, 30.

(4) Underwood, J. H.; Barbee, T. W. *Appl. Opt.* **1981**, *20*, 3027.

(5) Jin, B. Y.; Ketterson, J. B. *Adv. Phys.* **1988**, *38*, 189.

(6) Lakes, R. *Nature* **1993**, *361*, 511.

(7) Lurie, K. A.; Cherkaev, A. V. *Proc. R. Soc. Edinburgh* **1984**, *99A*, 71.

(8) Torquato, S. *Appl. Mech. Rev.* **1991**, *44*, 37−76.

(9) Aksay, I. A. *et al.* (Eds.) *Hierarchically Structured Materials,* MRS Proc. *255*, **1992**.

(10) (a) Ahuja, R.; Fraser, H. L. *J. Min. Met. Mater. Soc. (JOM)* **1994,** *46*, 35. (b) Aita, C. R.; Scanlan, C. M.; Gajdardziska-Josifovska, M. *J. Min. Met. Mater. Soc. (JOM)* **1994**, *46*, 40.

(11) Trau, M.; Saville, D. A.; Aksay, I. A. *Science* **1996**, *272*, 706−709.

(12) Ruess, F. F. *Mem. Soc. Imp. Natur. Moscou* **1809**, *2*, 327.

(13) Heavens, S. N. In *Advanced Ceramic Processing and Technology, Vol. 1*; Binner, J. G. P., Ed.; Noyes Publications: Park Ridge, NJ, 1990.

(14) (a) Pieranski, P. *Contemp. Phys.* **1983**, *24*, 25. (b) Pusey, P. N.; van Megan, W. *Nature* **1986,** *320*, 340. (c) Aastuen, D. J. W.; Clark, N. A.; Cotter, L. K.; Ackerson, B. J. *Phys. Rev. Lett.* **1986,** *57*, 1733. (d) Schatzel, K.; Ackerson, B. J. *Phys. Rev. Lett.* **1992**, *68*, 337. (e) van Megan, W.; Underwood, S. M. *Nature* **1993**, *362*, 616. (f) Okubo, T. *Langmuir* **1994**, *10*, 1695.

(15) (a) Onoda, G. Y. *Phys. Rev. Lett.* **1985**, *55*, 226. (b) Van Winkle, D. H.; Murray, C. A. *Phys. Rev. A* **1986**, *34*, 562. (c) Freeman, R. G.; *et al. Science* **1995**, *267*, 1629.

S0743-7463(97)00568-4 CCC: $14.00

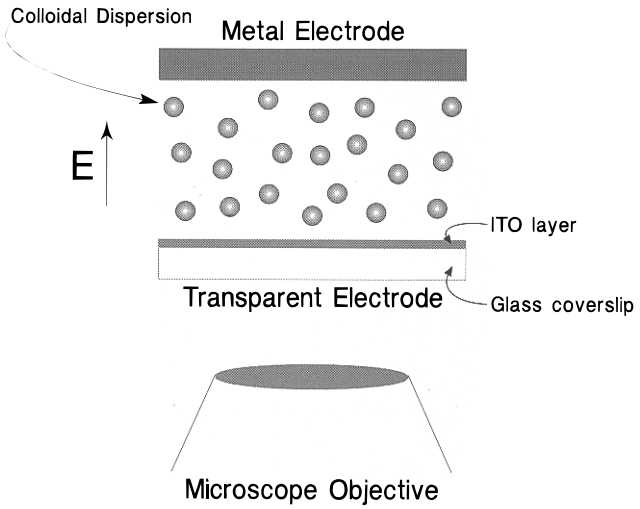

Figure 1. Schematic apparatus diagram.[11] The cell consists of an ITO-coated microscope coverslip (the anode) which is separated from the brass cathode by a 0.2 mm thick insulating Teflon spacer. The thin cavity is filled with a colloidal dispersion.

deposited layer. Indeed, it is generally assumed that the dynamics of electrophoretic layer formation are identical to those during particle sedimentation. For example, in their seminal paper,[16] *Hamaker* and *Verwey* state "the chief action of the electric field is in moving the particles towards the electrode and in producing a force which presses the particles together on the surface of the electrode in the same way as the force of gravity presses them on the bottom of a container." One of the aims of our work is to show that this is only part of the story. Moreover, it is widely understood that electrophoretically deposited layers are rather ramified. Another aim of this paper is to demonstrate that densely packed (crystalline) colloidal layers can be formed via electrophoretic deposition.

Experiment Discussion

To provide a basis for the theory to be described, it is helpful to recall salient points from our earlier work.[11] Similar observations were made with dc fields by Böhmer.[17] The electrophoretic deposition process takes place under conditions where, in the absence of an applied field, particles remain colloidally stable with respect to each other and an electrode surface. An optically transparent indium tin oxide (ITO) electrode and an optical microscope (Leitz Metallovert) were used to visualize the process. Figure 1 depicts the apparatus. The anode was a thin, vapor-deposited film of indium tin oxide on a glass microscope coverslip (60 Ω per square resistivity; Hampton Scientific); a 2 cm × 2 cm piece of polished brass serves as the cathode. Separation was provided by a 0.2 mm insulating Teflon spacer. Particles on or near the ITO electrode were viewed with a video camera and images recorded on videotape. Figure 2 shows an example of the electrophoretic deposition processes achieved with polystyrene particles (2 μm diameter size standards; Duke Scientific). Here the fluid contained a mixture of ionic and nonionic surfactants, added by Duke Scientific to ensure stability. Two-dimensional "gaseous" structures (plate a) formed upon applying a weak field (e.g., 0.5 V) across a dilute suspension or when the particles were allowed to sediment onto the electrode. Particles continued to move laterally via Brownian motion. The

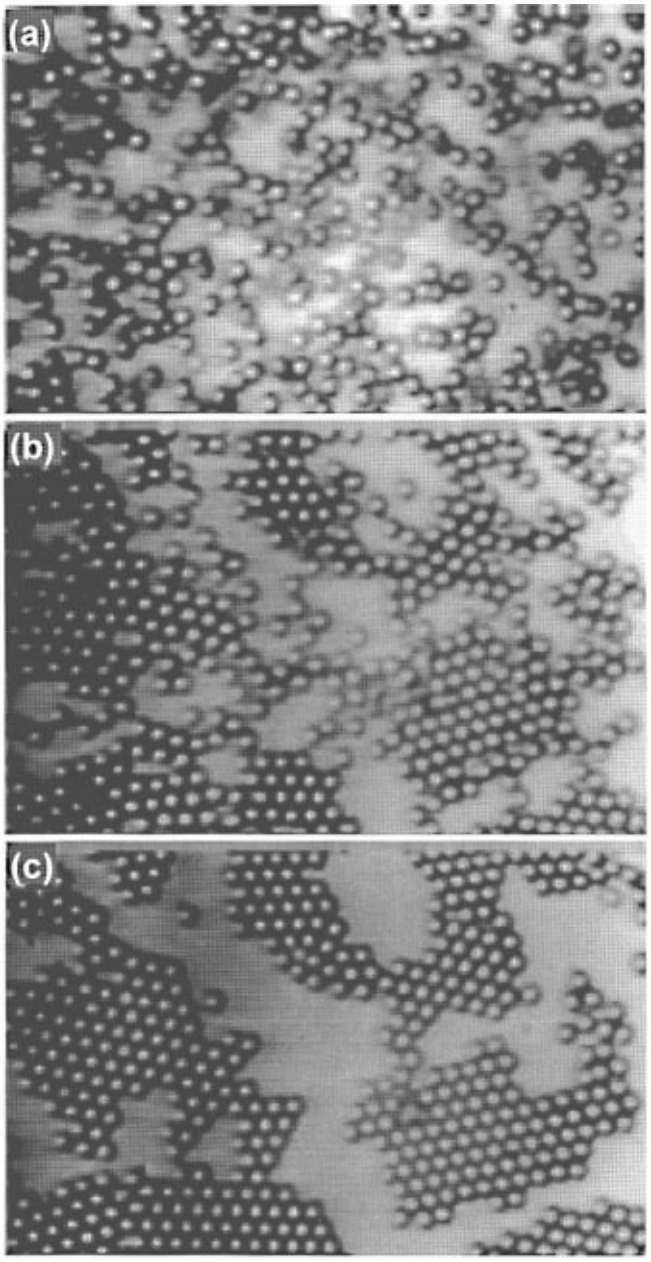

Figure 2. An example[11] of the long range lateral attraction which acts during electrophoretic deposition of 2 μm diameter polystyrene particles with a constant voltage (2 V). The long-range lateral attraction aggregates the particles into 2D crystals. The time elapsed between each frame is ~15 s. No field is applied in (a). Manipulating the current density changes the magnitude of the lateral attraction allowing the formation of different 2D colloidal phases: gaseous, liquid and solid. (Reprinted with permission from ref 11. Copyright 1996 American Association for the Advancement of Science.)

mobility of particles on the surface of the ITO electrode in the presence of an electric field is somewhat unexpected given the strong electrostatic attraction between negatively charged particles and the positive electrode. Stability appears to derive from steric effects provided by a surfactant layer on the polystyrene particles and a layer of polysilicate moieties on the silica particles.[11]

Increasing the applied voltage (e.g., from 0.5 to 1.5 V) produced interesting behavior (see parts b and c of Figure 2). In the presence of a sufficiently strong field, particles were observed to move *toward* one another across the surface of the electrode. This migration was transverse to the applied field and strong enough to lead to stable two-dimensional colloidal crystals. Lateral attraction of

(16) Hamaker, H. C.; Verwey, E. J. W. *Trans. Faraday Soc.* **1940**, *36*, 180.
(17) Böhmer, M. *Langmuir* **1996**, *12*, 5747.

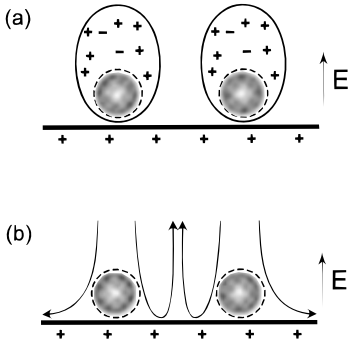

Figure 3. Schematic of particles near electrode surface: (a) polarization of double layer; (b) flow pattern expected to give rise to particle attraction.

this sort was first observed by Richetti *et al.*,[18] but a detailed theory was not provided. At field strengths between 50 and 100 V cm^{-1} (1−2 applied V), the process was reversible and, upon removing the applied field, Brownian motion quickly formed the "gaseous" structures shown in Figure 2a. The assembly process could be modulated by changing the amplitude of the applied electric field. Altering the strength of the interaction promoted different two-dimensional colloidal phases on the electrode, i.e., gaseous, liquid, and crystalline phases. Phase transitions were induced by varying the ionic current through the cell. The lateral attraction was also present with ac voltages at frequencies below approximately 1 MHz. Similar phenomena were observed with other particles, e.g., 16 nm gold particles and micrometer-size silica.[11]

The ability to externally modulate the magnitude of the lateral attractive interaction between electrophoretically deposited particles enables the controlled assembly of highly ordered mono- and multilayers. Manipulation of the process variables controls the size of the domains allowing formation of a variety of packing geometries, from amorphous to highly crystalline.[11]

Once the crystalline structures are formed, they may be "frozen" by inducing controlled coagulation with the applied field. For example, upon the application of a strong dc voltage (>2 V) the particles coagulate and permanently adhere to the electrode. Although the experiments have been performed with silica, polystyrene, and gold particles, this method of forming densely packed colloidal layers is by no means restricted to these materials. Indeed, provided the colloidal stability of the depositing particles can be maintained at the electrode, it should be possible to deposit many colloidal materials in a controlled manner.[11]

Attraction between electrophoretically deposited particles is unexpected due to the strong repulsion arising from electrostatic interparticle forces. The particles are similarly charged and possess a diffuse ion cloud (double layer), polarized by the applied field. Thus, nearby particles experience electrostatic repulsion from monopole and dipole interactions (see Figure 3a). Evidently, the migration of one particle toward another or toward a raft of particles is not the result of interparticle forces. Moreover, whatever the interaction, it must be strong enough to overcome electrostatic repulsion.

We suggest that the interaction results from electrohydrodynamic flows arising from the passage of ionic current through the solution. Measured currents lie between 1 and 500 μA cm^{-2}, depending on the applied potential difference and the time required to reach steady state. Although water electrolysis is present, bubble formation is never observed in our experiments because current densities are kept below 1 mA cm^{-2}.[19] This allows the H_2 and O_2 reaction products to be transported away from the electrode and solubilized into bulk solution. Other electrochemical reactions may contribute to the measured current; however, these are negligible because similar results are observed using transparent gold (10 nm thick gold film vacuum deposited onto a glass microscope coverslip) and carbon electrodes.

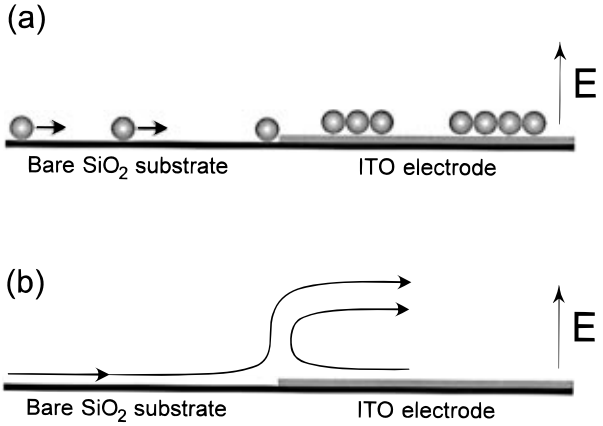

Figure 4. Schematic of electrode step: (a) lateral particle motion observed when a field is applied; (b) convective flow observed with AC field.

H_3O^+ and OH^- ions are formed, respectively, at the anode and cathode electrodes, and depending on the solution pH, these ions are consumed at the respective counter electrodes. The relevant anode reactions are

$$3H_2O \rightarrow 2H_3O^+ + {}^1/_2O_2 + 2e^- \quad \text{(acidic conditions)} \quad (1)$$

$$2OH^- \rightarrow H_2O + {}^1/_2O_2 + 2e^- \quad \text{(basic conditions)} \quad (2)$$

while at the cathode

$$2H_3O^+ + 2e^- \rightarrow 2H_2O + H_2 \quad \text{(acidic conditions)} \quad (3)$$

$$2H_2O + 2e^- \rightarrow 2OH^- + H_2 \quad \text{(basic conditions)} \quad (4)$$

The overall cell reaction is $H_2O \rightarrow H_2 + {}^1/_2O_2$, with no net creation or destruction of ionic species in the bulk. Ionic conduction occurs through electromigration of hydronium and hydroxyl ions. Provided the fluid remains motionless, electromigration of dissolved ionic species leads to a build up of electrolyte near the electrodes—*concentration polarization*.[20] At steady state, the polarizing effect of electromigration is balanced by diffusion so an electrolyte concentration profile is established at each electrode. The accumulation of ions sets up a pressure gradient resulting from Coulombic body forces due to free charge. Given the planar symmetry of the system, the induced pressure gradient is laterally uniform. A region of nonuniformity on an electrode, however, initiates convective flow. One example of such a flow is in electroplating reactions, where convective currents lead to patterned blemishes on the

(18) (a) Richetti, P.; Prost, J.; Barois, P. *J. Phys. Lett.* **1984**, *45*, L-1137. (b) Richetti, F.; Prost, J.; Clark, N. A. In *Physics of Complex and Supermolecular Fluids*; Safran, S. A., Clark, N. A., Eds.; Wiley: New York, 1987.

(19) Bockris, J. O.; Khan, S. U. M. *Surface Electrochemistry: A Molecular Level Approach*; Plenum: New York, 1993.

(20) Levich, V. G. *Physicochemical Hydrodynamics*; Prentice-Hall: Englewood Cliffs, NJ, 1962.

plated surface.[21] We postulate that in our system, convection similar to that illustrated in Figure 4b ensues when the uniformity of the concentration polarization is disrupted by a colloidal particle. Lateral variations in the amount of concentration polarization induce a spatially varying "free charge", and the action of an electric field on the free charge produces fluid motion. Once motion is initiated, the charge density is further influenced by convection. The flow pattern illustrated in Figure 4b, for example, could bring particles together via an electrohydrodynamic interaction. Electrohydrodynamic motion of this sort accords with the long-range nature of the lateral migration where like-charged particles are carried by the flow. A quantitative theory of flow patterns near the electrode surface is presented later.

None of the other mechanisms for particle attraction advanced to date explains the observed long-range movement. For example, an excess of H_3O^+ or background electrolyte ions near the anode may reduce the electrostatic repulsion between the particles, by affecting the acid/base equilibrium of ionizable surface moieties, or screening the charge interactions between particles. These two effects would reduce electrostatic repulsion and allow lateral agglomeration of particles via van der Waals attraction. Such a mechanism does not explain the long range phenomena (>5 particle diameters) because van der Waals attractive forces for colloids operate on much smaller length scales (usually <1 particle diameter).[22] Moreover, migration is relatively insensitive to the composition and surface of the particles, e.g., very similar assembly processes are observed for both silica and polystyrene particles[11] even though the nature of charge on each of these is remarkably different. Although van der Waals attraction operates during electrophoretic deposition, it is not dominant until particle separation distances are small.

Another possibility is attraction stemming from purely electrokinetic effects such as electro-osmosis.[23] Our experiments with ac fields stand in opposition to this mechanism, however. Electrokinetic processes giving a net translation should be negligible above frequencies of 100 Hz, but we observed clustering at frequencies approaching 1 MHz.

Electrohydrodynamic flows typically stem from induced charge effects. Since the induced charge is proportional to the field, the electrical body force goes as the square of the field. Flow arises to produce viscous stresses to balance electrical forces. To establish the presence of electrohydrodynamic flow, experiments were performed with patterned electrodes. A simple arrangement is shown in Figure 4, where an electrode step was formed by removing part of the conductive ITO layer (with HCl) while protecting the remainder with an etch resistant polymer (later removed with a solvent wash). One side of the step is conducting, the other insulating. When an electric field is applied, a current gradient sets up across the step (approximately 5 μm in width). In rough terms, the electrode step geometry is a one-dimensional analogue of current variations near a spherical colloidal particle where gradations arise because the particle alters the field and the conductivity.

The effects of a one-dimensional gradient were demonstrated in an experiment similar to that shown in Figure 2. Initially particles are evenly distributed on either side of the step; cf. Figure 4a. Upon application of the field, particles on the nonconducting side of the electrode immediately move toward the conducting side. Long range lateral motion is observed more than 2 mm from the electrode edge. Both dc and ac fields were used and particle velocities of the order of several micrometers per second could be controlled by field strength or frequency. However, at frequencies above 1 MHz, no motion is observed. On the conducting side of the electrode, particles formed crystalline clusters in a manner similar to that shown in Figure 2. Clearly, an inhomogeneous current induces an electrohydrodynamic flow.

To further test this idea, and visualize motion, the experiment illustrated in Figure 4b was performed. Again 2 μm polystyrene particles were dispersed evenly on either side of the electrode step. After a small fraction was allowed to settle on the substrate, a 1 kHz, 10 V, ac field was applied. When particles near the substrate began to move, the focal plane of the microscope was changed to enable visualization of particle motion in bulk solution. At these frequencies, no electrophoretic translation is evident, so particles are influenced only by Brownian and convective forces and they act as tracers. Figure 4b illustrates the direction of fluid motion observed under these conditions. A convective flow pattern was established in the cell with fluid swept across the electrode step, up into the bulk solution, and recirculated. Visualization of the flow in this manner provides direct evidence of flow induced by the electrohydrodynamic mechanism.

Electrohydrodynamics

In the situations just described, fluid motion arises from electrical body forces acting on "free charge" generated in solution. To study such flows, we analyze a simple system, an electrochemical cell with parallel electrodes. At steady state, the rate of electromigration of background electrolyte is exactly balanced by the rate of diffusion and the current occurs solely through electromigration of H_3O^+ and OH^- species generated at the electrodes via the reactions described in eqs 1−4. The analysis is done in two stages. First we examine the basic one-dimensional fields of potential and concentration. Then, effects due to lateral modulation of these fields are studied via a perturbation analysis. This describes the space charge distribution and the electrical body forces. These are incorporated into the equations for Stokes flow to describe the structure of the circulation.

For reasons of mathematical simplicity, the model studied here differs somewhat from the actual experimental setup. Thus, we choose to ignore the ionization of water and focus on current near the cathode[24] in an acidic solution. This yields expressions which can be treated more-or-less analytically and simplifies the analysis tremendously, while preserving the essential physical processes.

Under acidic conditions, the electrode reactions are given by eqs 1 and 3, so the current is carried by hydronium ions. Following Levich,[20] an expression for the hydronium ion flux in the absence of convection is

(21) (a) Fleury, V.; Kaufman, J. H.; Hibbert, D. B. *Nature* **1994**, *367*, 435. (b) Wang, M.; van Enkevort, W. J. P.; Ming, N.; Bennema, P. *Nature* **1994**, *367*, 438. (c) Livermore, C.; Wong, P. *Phys. Rev. Lett.* **1994**, *72*, 3847.

(22) Russel, W. B.; Saville, D. A.; Schowalter, W. R. *Colloidal Dispersions*; Cambridge University Press: Cambridge, 1989.

(23) Electrokinetic effects such as electro-osmosis stem from deformation of the equilibrium diffuse layer.

(24) The experiments were carried out under acidic conditions brought about by the adsorption of atmospheric CO_2 to form carbonic acid. This electrolyte, hydronium and hydroxyl ions from water, and indifferent electrolyte ions from the colloidal suspension further complicate matters and thwart an exact analysis.

(25) For our experiments, $I \approx 100\ \mu A/cm^2$, $n_\infty \approx 0.1$ mM, $\omega^1 \approx 2 \times 10^{11}$ m/(N s), so $l_p \approx 10\ \mu$m.

$$j^1 = -e\omega^1 n^1 \frac{\partial \varphi}{\partial y} - \omega^1 k_B T \frac{\partial n^1}{\partial y} \quad (5)$$

with y denoting distance from the electrode. Polarization effects arise from the presence of a single 1−1 electrolyte, viz.

$$j^2 = -e\omega^2 n^2 \frac{\partial \varphi}{\partial y} - \omega^2 k_B T \frac{\partial n^2}{\partial y} = 0 \quad (6)$$

$$j^3 = +e\omega^3 n^3 \frac{\partial \varphi}{\partial y} - \omega^3 k_B T \frac{\partial n^3}{\partial y} = 0 \quad (7)$$

where j^1 is ionic flux of H_3O^+, j^2 is the cation flux, and j^3 is the anion flux. Since hydronium ions are consumed at the cathode, $j^1 < 0$ and the current $I = -ej^1$, φ represents the electrostatic potential at a distance y from the electrode, ω^κ is the mobility, and n^k is the concentration of the kth ionic species, while k_B and T stand for Boltzmann's constant and temperature, respectively. The relation between charge and potential is

$$\epsilon\epsilon_0 \frac{\partial^2 \varphi}{\partial y^2} = -e(n^1 + n^2 - n^3) \quad (8)$$

with e as the charge on a proton, ϵ as the dielectric constant of the solvent, and ϵ_0 as the permittivity of free space.

It is helpful to carry out a scale analysis of the equations. The dimensional variables are replaced by dimensionless variables according to the scheme

(dimensional variable) → (scale factor) (dimensionless variable)

Choosing scale factors of k_BT/e (potential), n_∞ (concentration), $l_p \equiv en_\infty\omega^1 k_B T/I$ (distance),[25] and ω^1 (mobility), produces

$$1 = n^1 \frac{\partial \varphi}{\partial y} + \frac{\partial n^1}{\partial y} \quad (9)$$

$$0 = -\omega^2 n^2 \frac{\partial \varphi}{\partial y} - \omega^2 \frac{\partial n^2}{\partial y} \quad (10)$$

$$0 = +\omega^3 n^3 \frac{\partial \varphi}{\partial y} - \omega^3 \frac{\partial n^3}{\partial y} \quad (11)$$

$$\lambda \frac{\partial^2 \varphi}{\partial y^2} = -(n^1 + n^2 - n^3) \quad (12)$$

with $\lambda \equiv \epsilon\epsilon_0 k_B T/e^2 n_\infty l_p^2$. For our experiments, $\lambda \approx 10^{-6}$. Accordingly, electroneutrality prevails locally. For the indifferent electrolyte

$$n^2 = c^2 \exp(-\varphi) \quad (13)$$

$$n^3 = c^3 \exp(\varphi) \quad (14)$$

From these equations we find

$$\varphi = \ln\left[1 + \frac{y}{2c^3}\right] \quad (15)$$

Here φ represents the dimensionless potential scaled so $\varphi = 0$ at $y = 0$.

(26) Here we use complex notation with the understanding that only real parts will be used in the final result. The index i denotes $\sqrt{-1}$.

From the expressions for the potential and ion concentrations near the electrodes, we can estimate pressure distribution from the charge density, ρ^f, and the field strength in the y-direction, E, as follows. The equation for hydrostatic equilibrium in terms of dimensional variables is

$$-\frac{dp}{dy} + \rho^f E = 0 \quad (16)$$

Since the expressions derived represent the leading terms in series expansions of the form

$$\text{potential} \sim \frac{k_B T}{e}[\varphi + \lambda\psi + O(\lambda^2)]$$

$$\text{ion concentration} \sim n_\infty[n^i + \lambda m^i + O(\lambda^2)] \quad (17)$$

the dimensional charge density, ρ^f, is $-en_\infty\lambda\nabla^2\varphi$ where $\lambda \ll 1$. Accordingly, in dimensionless terms,

$$-\frac{dp}{dy} + \lambda \frac{d^2\varphi}{dy^2}\frac{d\varphi}{dy} = 0 \quad (18)$$

with the pressure scale being $n_\infty k_B T$. This shows that the dimensionless pressure is $O(\lambda)$. The expression for the potential shows that pressure increases as one moves away from the electrode. However, as long as the potential (and therefore the charge) is laterally uniform, the fluid remains motionless. During electrophoretic deposition, current gradients across the electrode surface develop because of the shielding effect of particles. Fluid motion ensues when the laterally uniform charge distribution is disrupted and viscous stresses arise to balance the lateral electric stresses.

To describe fluid motion resulting from the concentration polarization mechanism, the model is simplified by restricting attention to regions near electrodes. This allows analytical treatment. First, we estimate the size of the velocity induced by lateral perturbations due to the particles. A particularly simple way of seeing things is to recognize that lateral variations in the current lead to pressure variations which are in turn balanced by flow. Suppose the fractional change in l_p is δ. Then the pressure variation over a distance Δx, say, must be balanced by viscous stresses caused by flow of a liquid with viscosity, μ, so

$$\Delta p \approx \mu u \Delta x/(l_p)^2 \quad (19)$$

and the velocity is

$$u \approx n_\infty k_B T (l_p)^2 \lambda\delta/\mu\Delta x \quad (20)$$

Using the numerical data already given yields a velocity of over 10δ μm/s when $\Delta x = l_p$. Evidently substantial flows can be induced by current variations of a fraction of a percent.

The structure of the flow field is calculated as follows. From the expression for the electrostatic potential near the cathode, the equilibrium pressure field is calculated. Then a small perturbation is introduced and the structure of the perturbed fields is determined. The perturbed potential and charge fields enable us to calculate the electrical body force in the Stokes equations used to describe fluid motion. Since no allowance is made for the effect of convection on the ion distribution, this represents only the initial stage of the electrohydrodynamic flow. Nevertheless, it gives a clear picture as to the mechanism

behind fluid motion. Detailed calculations will be required to establish the model quantitatively.

A perturbation method is used to calculate the velocity profile for flow induced by current variations across the electrode surface. The situation near a cathode will be analyzed here to avoid singularities in the analytical expression for the potential. Since the problem is linear, only one harmonic is needed,[26] viz.

$$I^{**}[1 + \delta \exp(ikx)] \tag{21}$$

where I^{**} represents current density at a reference point on an electrode, x is distance along the electrode surface scaled on l_p, δ is an arbitrary (small) constant, and $k = 2\pi l_p/L$, where L is the wavelength of the perturbation. Accordingly, the concentration fields of electrolyte species and the electrostatic potential are represented[27] as

$$N^j(x,y) = n^j(y) + \delta f_j(y) \exp(ikx) \tag{22}$$

$$\Phi(x,y) = \varphi(y) + \delta f_4(y) \exp(ikx) \tag{23}$$

The f-functions depend solely on y and describe the effect of the perturbation.

Use of eq 22 for $j = 1$, 2, and 3 and eq 23 in conservation laws for the ions leads to a coupled set of differential equations which may be solved analytically. The expression for f_4, the perturbation potential,[28]

$$f_4 = K_0\left[2kc^3\left(1 + \frac{y}{2c^3}\right)\right] \tag{24}$$

Next, the Stokes equations are used to represent the balance between viscous stress, pressure, and electrical forces, viz.

$$\mathbf{0} = -\nabla p + \rho^f \mathbf{E} + \mu\nabla^2\mathbf{u} \quad \text{and} \quad \nabla\cdot\mathbf{u} = 0 \tag{25}$$

Guided by the previous calculations, these equations are made dimensionless by scaling lengths with $2c^3l_p$, pressures with $n_\infty k_B T\lambda$, and velocity with $n_\infty k_B T 2c^3 l_p \lambda/\mu$. Recall the scale for potential is $k_B T/e$ and the charge is $-en_\infty\lambda\nabla^2\Phi$. Then, since the problem is two-dimensional, a stream function, ψ, can be used to represent the (dimensionless) flow field as

$$u_x = \frac{\partial\Psi}{\partial y}; \qquad u_y = -\frac{\partial\Psi}{\partial x} \tag{26}$$

$$\Psi(x,y) = \delta f_5(y) \exp(ikx) \tag{27}$$

Substitution of eqs 26 and 27 into the Stokes equations produces a fourth-order differential equation

$$f_5'''' - 2k^2 f_5'' + f_5 = ik\left[(f_4'' - k^2 f_4)\frac{d\phi}{dy} - f_4\frac{d^3\phi}{dy^3}\right] \tag{28}$$

Primes denote differentiation with respect to y. A particular solution of eq 28 was constructed by *variation of parameters*, calculating the required integrals numerically with boundary conditions which make the perturbation vanish at the electrode and far away, i.e., $f_5(0) = f_5(\infty) = f_5'(0) = f_5'(\infty) = 0$. Taking the real part of the general solution gives the dimensionless fluid velocity components as

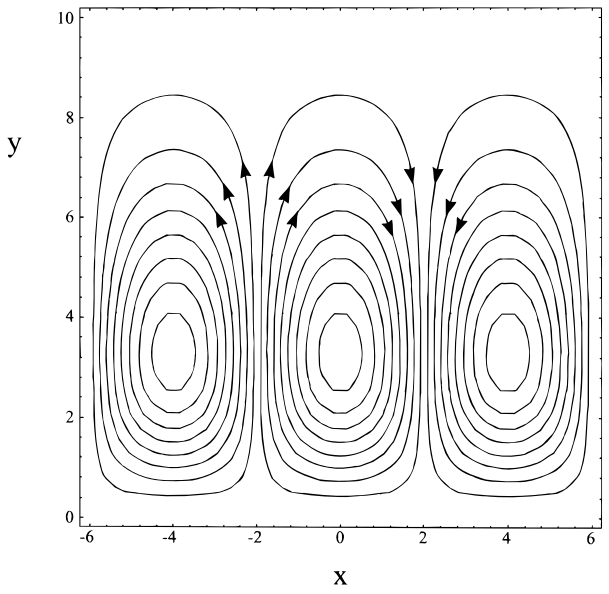

Figure 5. Streamline pattern for flow generated near the electrode surface by a periodically varying current density with $k = \pi/4$ (wavelength $= 16c^3l_p$). The arrows denote the direction of flow.

$$u_x = \delta\frac{\partial f_5(y)}{\partial y}\cos(kx) \tag{29}$$

and

$$u_y = \delta\, k\, f_5(y) \sin(kx) \tag{30}$$

The strength of the velocity depends on the concentration polarization thickness, increasing with increased current density and decreasing with increased background electrolyte concentration.

Figure 5 depicts the structure of the flow pattern near the electrode interface with a periodically varying current density where $k = \pi/4$. These cells represent a quantitative prediction of the schematic flow patterns discussed previously (see Figure 4). Although the cells fill the space between the electrodes, flow is weak outside the polarization layer. According to the figure, lateral flow is strongest where the current is either high or low, implying that particles will be swept into regions between. This accords, qualitatively, with the observed behavior. Nevertheless, these remarks must be tempered by the fact that, as noted earlier, these calculations related only to the initial instant inasmuch as once motion begins, the concentration fields are distorted by flow.

Although our calculations pertain to a particular steady state, the form of the electrical body force yields insight into behavior in an oscillatory field. Suppose, for example, the electrode potential varies periodically as $\cos(\bar{\omega}t)$. Since the electrical body force is proportional to the square of the potential, the body force will vary as $\cos^2(\omega t) = {}^1/_2[1 + \cos(2\tilde{\omega}t)$ yielding a nonzero average force. Of course, the steady part will depend on the frequency in a complicated way. The details are obscure, but it is clear that an electrohydrodynamically driven motion will exist in an oscillatory field. Presently, we do not have a satisfactory explanation for the disappearance of the phenomenon above 1 MHz. A variety of steady and oscillatory motions have been studied in other contexts.[29−32]

(27) The index $j = 1$ denotes the hydronium ion, $j = 2$ and 3 stand for indifferent anions and cations, respectively.
(28) $K_0[\cdot]$ denotes a modified Bessel function.
(29) Taylor, G. I. *Proc. R. Soc. London* **1966**, *A291*, 159.
(30) Saville, D. A. *Phys. Rev. Lett.* **1993**, *71*, 2907.
(31) Trau, M., Sankaran, S., Saville, D. A., Aksay, I. A. *Langmuir* **1995**, *11*, 4665.

Conclusions

A mechanism for colloidal assembly at electrode interfaces has been demonstrated. During electrophoretic deposition, particles are influenced by a long-range process strong enough to assemble the particles into two-dimensional crystalline aggregates. The lateral motion is a general phenomenon which occurs for any type of colloidal material located near an electrode surface, provided colloidal stability is maintained. The processes have been observed to operate on depositing particles ranging in size from 16 nm to 2 μm in diameter, with both dc and ac fields.[11] Lateral migration appears to result from an electrohydrodynamic mechanism wherein gradients in current density, caused by the presence of particles near the electrode surface, generate localized fluid flow. Calculations based on this model accord with flow patterns observed near etched "step electrodes", where large-scale convective cells are generated as a result of a current gradients. External manipulation of the lateral attraction, by varying either field strength or frequency, allows the reversible formation of a variety of two-dimensional colloidal states on the electrode surface, e.g., gaseous, liquid-like, or crystalline states. Further manipulation facilitates the assembly of crystalline multilayers or more complicated "designed" structures. Once the required colloidal structures are assembled, they may be permanently frozen into place by controlled coagulation with the applied field. We believe the simplicity of this assembly method makes the approach very attractive as a route to economically manufacture nanostructured materials. This method may also be suitable as a way to assemble complex macromolecules such as proteins into two-dimensional crystals or other patterned configurations.

Acknowledgment. This work was supported by the Army Research Office, Multidisciplinary University Research Initiative (ARO/MURI) (Grant DAAH04-95-1-0102) (M.T. and I.A.A.), the Microgravity Science and Applications Division of NASA (D.A.S.), and the National Science Foundation (DMR-940032) (M.T.). Partial support for M.T. was provided by the Fulbright Commission. We acknowledge discussions with A. B. Bocarsly.

LA970568U

(32) Saville, D. A. *Annu. Rev. Fluid Mech.* **1997**, *29*, 27.